Journal of Electrical and Electronic Engineering
2023; 11(4): 82-88
http://www.sciencepublishinggroup.com/j/jeee
doi: 10.11648/j.jeee.20231104.11
ISSN: 2329-1613 (Print); ISSN: 2329-1605 (Online)

Modelling of Current Transport Mechanisms in GaSb-Rich Type-II Superlattice Infrared Photodiodes

Vishnu Gopal[1], Raghvendra Sahai Saxena[2]

[1]Institute of Defence Scientists and Technologists, Delhi, India

[2]Solid State Physics Laboratory, Delhi, India

Email address:

vishnu_46@yahoo.com (Vishnu Gopal), rs_saxena@yahoo.com (Raghvendra Sahai Saxena)

To cite this article:

Vishnu Gopal, Raghvendra Sahai Saxena. Modelling of Current Transport Mechanisms in GaSb-Rich Type-II Superlattice Infrared Photodiodes. *Journal of Electrical and Electronic Engineering*. Vol. 11, No. 4, 2023, pp. 82-88. doi: 10.11648/j.jeee.20231104.11

Received: July 3, 2023; **Accepted**: August 5, 2023; **Published**: August 15, 2023

Abstract: In this paper we propose an alternative approach to model the performance limiting current leakage mechanism in GaSb-rich type II superlattice diodes than reported earlier. The reported conclusions are based on the analysis of the current – voltage (I – V) and dynamic resistance – voltage (R_d – V) characteristics of these diodes. None of the carrier transport parameters evaluated from independent measurements on similar samples are used in the present analysis as some of the material parameters like carrier concentrations and mobilities are evaluated by Hall measurements along the planes parallel to the deposited layers constituting the superlattice, whereas the transport of carriers in practical superlattice diodes takes place in the vertical direction. Instead, we have used a method which extracts the desired parameters from the measured I – V itself. Our analysis has shown that the GaSb-rich superlattice diode's performance limiting leakage current mechanism is the contribution from surface leakage currents, which have been modelled as shunt current that is of ohmic nature in low reverse bias region near zero-bias. The same leakage current however grows in its own proportion leading to an exponential increase of the leakage current in the higher reverse bias region. The reverse bias region corresponding to the exponential increase of the leakage current exhibits consequent degradation in the dynamic resistance of the diode leaving behind a peak in the dynamic resistance characteristic. The reverse bias voltage corresponding to the peak dynamic resistance is the limiting bias voltage for the ohmic behaviour of the shunt current.

Keywords: Superlattice Diode, GaSb-Rich, (I – V) Characteristics, Dynamic Resistance Characteristics

1. Introduction

The results of simulations of the current-voltage (I – V) characteristics of type II GaSb-rich superlattice mid-wave infrared (MWIR) photodiodes were reported [1] recently by using ATLAS software from SILVACO. This software essentially uses a bulk model based on the effective band gap of superlattice material. The software further requires the advance knowledge of the several material parameters like carrier concentrations, mobility, lifetime of minority carriers etc. from independent measurements. Alternatively, some of these parameters, if not known are used as fitting parameters. Delmas et. al. [1] in their investigation have reported the main performance limiting leakage current mechanism of the GaSb-rich superlattice diodes as trap-assisted-tunnelling currents on account of the traps contributed by the defects in GaSb-rich superlattice structures. In addition, they have also highlighted the presence of an electric field that breaks the mini bands in to localized Wannier–Stark states and contribute to the strong tunnelling currents at low reverse bias. The latter tunnelling currents were invoked to reconcile the two orders of magnitude disagreement between the minority carrier lifetime used in the fitting of I-V characteristics and the minority carrier lifetime of the GaSb-rich superlattice structure evaluated from the independent time resolved photoluminescence measurements. In this connection it is worth mentioning here that these type II superlattice structures have highly anisotropic nature of the band structure and the resulting modified density of states leads to the transport of carriers that may be quite different from bulk isotropic systems [2].

We, in this paper, intend to use a method, which extracts the desired information on the transport parameters of the

GaSb-rich superlattice IR photodiode from its measured I–V characteristics itself. The analysis of the I–V characteristics and dynamic resistance–voltage (R_d–V) characteristics show that the surface leakage current, which is essentially the shunt current, is the dominant current mechanism that limits the performance of these diodes. This analysis further shows that the entire I–V and R_d–V characteristics of these diodes can be very well accounted for without invoking the generation – recombination (g–r) and tunnelling currents. Non-ideal nature of the forward characteristics of the diode that lead to an ideality factor of more than unity is assigned to the contributions from the shunt / surface leakage currents [3, 4]. The reverse bias characteristics of these diodes appear to be dominated by a process in which the current grows in its own proportion leading to an exponential increase of the shunt current in the medium and high reverse bias voltage range. The low reverse bias region near zero-bias confirms to our current knowledge of the ohmic shunt behaviour of surface leakage currents.

This method allows quickly analysing not only a photodiode behaviour but also the nonuniformity in the photodiode array. Being a simple algebriac model with numerical robustness and better computational efficiency with respect to the conventional models [6-12], this may be used to model the behaviour of photodiode arrays with practically observed nonuniformity in their electrical characteritics for use in the circuit simulation of readout integrated circuit (ROIC) to ensure good matching and compatibility between detector arrays and ROIC, leading to the development of IR focal plane array technology [5, 6].

2. Physical Model

In the past the bulk-based models [7-13] that use effective band gap of super-lattice material have been used to analyse the electrical characteristics by including diffusion, generation-recombination (g-r), trap-assisted-tunnelling, band-to-band tunnelling and shunt currents as the operating transport current mechanisms within these types of super-lattice diodes. The present paper however show that the principal transport current mechanisms operating within the diodes are the thermal diffusion of minority carriers to the junction and surface leakage currents in addition to the diffusion of background generated minority carrier current (photocurrent) to the junction. Brief description of the transport currents in the following paragraphs is therefore limited to the thermal diffusion and shunt currents in addition to the background generated photo-current, which accounts for the finite current of the diode at zero-bias.

2.1. Diffusion Current

It is the most fundamental component of the diode current that arise due to the diffusion of thermally generated minority carriers from the quasi-neutral n- and p- regions to the junction. The thermal diffusion current of an ideal dark p-n junction diode is given by the following equation,

$$I_{dif} = I_{sat}\left[\exp\left(\frac{qV}{KT}\right)-1\right] \quad (1)$$

I_{sat} is the reverse bias saturation current of the diode. Its numerical magnitude is dependent on the various material and diode parameters like doping concentrations on the p and n-side of the junction, the intrinsic carrier concentration in the base material, diode's junction area and the bias voltage, the thickness of the p and n-regions of the diode, electron and hole lifetimes, the electron and hole mobilities and the electron and hole diffusion lengths of the diffusing minority carriers from either side of the junction. The mathematical equation that describes the relationship of the material parameters with the diode saturation current, I_{sat} is available in all standard text books on semiconductor devices and is not repeated here. Moreover, the present work is not making use of this relationship or independently known values of any of the material parameters.

The gate-controlled diode experiment [3] followed by the presentation of a physical model has shown that the surface leakage currents induce non-ideal I-V characteristics in a diode [4]. The forward non-ideal I-V characteristic can be very well described by the following modified form of Eq. (1),

$$I_{dif} = I'_{sat}\left[\exp\left(\frac{qV}{\eta KT}\right)-1\right] \quad (2)$$

where η is the ideality factor of the diode, whose value is nearly unity in the absence or negligibly low surface leakage current. Higher values of the surface leakage current in a given diode lead to the values of η more than unity [3, 4]. Unlike the g-r theory of Sah, Noyce and Shockley (SNS) [14], η may exceed even 2 depending upon the magnitude of surface leakage currents [3, 4]. Here, I'_{sat} is the thermal saturation current of the diffused charge carriers in presence of surface leakage [4] and is higher than the reverse saturation current I_{sat} of an ideal diode.

2.2. Effect of Finite Zero-Bias Current

Diodes fabricated from narrow bandgap materials like Mercury Cadmium Telluride or superlattice material are generally mounted for the measurements of their electrical characteristics on a cooled stage inside a vacuum enclosure [15]. Most often diode receives some IR radiation from the surrounding background objects including the walls of vacuum enclosure due to imperfect cold shielding of the diode. Even in those cases where measurements are made by immersing the diode in say, liquid nitrogen container / Dewar, some IR radiation from the background is still received by the diode as liquid nitrogen is not fully opaque to the incident IR radiation from the background. The photo-current I_{Ph} generated by this undesired IR radiation from the background objects is essentially the minority carrier current, which diffuse towards the junction and is observed as the finite zero-bias current of the diode. Its effect on the I-V

characteristic of the diode can be taken in to account by suitably modifiying Eq. (2) in the following form.

$$I_{dif} = I'_{sat}\left[\exp\left(\frac{qV}{\eta KT}\right)-1\right]-I_{Ph} \quad (3)$$

In general, the net effect of the background radiation on the current characteristics is to shift its I–V curve along current axis towards the negative values of the current by an amount equal to the photo-excited minority carrier current I_{Ph}. This shift results in a cross over of the I–V characteristcs with the voltage axis at certain positive voltage, known as the open circuit voltage, V_{OC} that may be derived from Eq. (3) as an estimate of the forward voltage corresponding to the zero current, as follows:

$$V_{OC} = \frac{\eta KT}{q}\ln\left[\frac{I_{Ph}}{I'_{sat}}+1\right] \quad (4)$$

In practice it is however possible that a smaller value of I_{Ph} or a higher value of thermal saturation current I'_{sat} give rise to a small open circuit voltage that may not be observable if the measurement interval of applied bias voltage is higher than the resulting open circuit voltage. In this kind of situation both η and V_{OC} may be treated as variable fitting parameters to fit the forward characteristics of the diode to Eq. (3). The required value of I'_{Sat} to complete the fitting of the forward current characteristic to Eq. (3) can be obtained from the following relation for the chosen values of η and V_{OC},

$$I'_{sat} = \frac{I_{Ph}}{\exp\left(\frac{qV_{OC}}{\eta KT}\right)-1} \quad (5)$$

It has been shown in previous reports [3, 16-18] that Eq. (3) provides an excellent fit to the forward characteristics of the diodes if the proper care is taken to include the series resistance of the diode by using the following expression,

$$V_{appl} = V + I_{dif}.R_{sr} \quad (6)$$

where V_{appl} is the externally applied bias voltage, V is the voltage across junction and R_{sr} is the series resistance of the diode.

2.3. Shunt Current

I-V characteristics of an un-passivated or imperfectly passivated diode contain a current component known as surface leakage current, which is often modelled as an ohmic shunt current by applying Ohm's law, i.e.,

$$I_{Sh} = \frac{V}{R_{Sh}} \quad (7)$$

where V is the bias voltage across the diode and R_{Sh} is the diode's shunt resistance. The surface leakage currents and the dislocations in the material which intersect the junction [19, 20] are generally held responsible as the possible sources of ohmic shunt current. The contribution of ohmic shunt currents from the two sources is not easily distinguishable. It is therefore modelled as gross contribution.

The calculation of the shunt current as a function of applied bias voltage requires knowledge of the shunt resistance of the diode, which may be estimated by computing the diode's dynamic resistance (dV/dI) as a function of bias voltage. The highest (peak) value of dynamic resistance is the unique point in the entire dynamic resistance plot, where dR/dV is zero. Zero value of dR/dV physically signifies a resistance that is independent of the applied voltage. It is known that an ohmic shunt resistance too, is independent of the applied voltage. To a first approximation the diode resistance corresponding to dR/dV = 0 may be thus considered as a good estimate of the ohmic shunt resistance of the diode.

Alternatively, in those cases where shunt current is the dominant current of the diode, it should be possible to estimate the ohmic shunt resistance by fitting the measured current variation at low reverse bias voltages near zero-bias to the ohm's law as the diode current in excess of diffusion and photo-currents confirms to the ohm's law in this bias region.

2.4. Excess Current

It has been reported in the past [3, 16-18, 21] that the sum of thermal diffusion current, background photo-current and ohmic shunt current provides good fit to the reverse bias I–V characteristics over a limited range of small reverse bias voltages beginning from zero-bias as the small surface leakage currents only confirm to the ohmic current model. At higher reverse bias voltages, the diode current however exhibits an excess current, which is dependent on the magnitude of the shunt resistance / shunt current of the diode under investigation. Lower the shunt resistance, higher is the excess current. The excess current at higher reverse bias voltages has been found to be described by the following expression due to the nonlinear behaviour of the shunt resistance [3, 16-18, 21].

$$I_{excess} = I_{r0} + K_1\exp(K_2 V) \quad (8)$$

I_{r0}, K_1 and K_2 are the constants that are obtained by fitting the diode's excess current in the reverse bias to Eq. (8). Fitting always leads to the positive value of I_{r0} and a negative value of K_1. This shows that during the growth of excess current both majority and minority carriers are produced. The exponential term representing the growth of minority carrier current can be mathematically obtained by assuming the growth of excess current in its own proportion,

$$\frac{dI_{excess}}{dV} = K_2 I_{excess} \quad (9)$$

or,

$$\int_{I_{th}}^{I_{excess}} \frac{dI_{excess}}{I_{excess}} = \int_{V_{th}}^{V} K_2 dV \quad (10)$$

In Eq. (10), K_2 is the constant of proportionality. V_{th}, the lower limit of integration on the R.H.S. of Eq. (10) is the threshold voltage above which the excess current grows in its own proportion. The corresponding lower limit of integration I_{th} on the L.H.S. is the excess thershold current that grows in its own proportion above the threshold voltage. Eq. (10) leads to the exponential term of Eq. (8). The value of the constant K_1 in Eq. (8) is related to I_{th} and V_{th} by the following relation,

$$K_1 = I_{th} \exp(-K_2 V_{th}) \tag{11}$$

Note that K_1 is also a constant since I_{th}, V_{th} and K_2 are all constants for a given diode. Eq. (8) can be thus used directly to fit the excess current of the diode without having known the values of V_{th} and I_{th}.

According to the above discussions the reverse bias current of the diode at small reverse bias voltages near zero-bias will be given by,

$$I_1 = I_{dif} + I_{Ph} + I_{Sh}(\text{ohmic}) \tag{12}$$

At higher reverse bias voltages, where shunt resistance / shunt current exhibits nonlinear behaviour the diode current is given by,

$$I_2 = I_{dif} + I_{Ph} + \left[I_{r0} + K_1 \exp(K_2 V) \right] \tag{13}$$

In addition to studying I–V characteristics of the diode to characterize the current transport mechanisms, this paper proposes to include the study of the variations in the differential resistance of the diode as a function of applied bias voltage, i.e., R_d–V characteristics, too. The variations in the differential resistance with respect to the applied bias voltage are much more sensitive to the small changes in the diode current responsible for the observed impedance than the total current by itself. The following paragraph will summarize the calculation of the resultant dynamic differential resistance of the diode based on the same current mechanisms that are used to characterize the I–V characteristics.

2.5. Dynamic Impedance of the Diode

Contribution of the thermal diffusion currents of the diode to its dynamic impedance (R_{dif}) is given by the following expression,

$$R_{dif} = \frac{\eta KT}{q I'_{sat}} \exp\left(-\frac{qV}{\eta KT} \right) \tag{14}$$

The above relation has been obtained from the differentiation of Eq. (3). Next, the contribution of excess current to the dynamic impedance of the diode obtained from differentiation of Eq. (8) is as follows,

$$R_{excess} = \frac{\exp(-K_2 V)}{K_1 K_2} \tag{15}$$

Above Eq. (15) essentially represents the nonlinear contribution of the shunt resistance at higher reverse bias voltages.

Estimation of the ohmic shunt resistance R_{Sh} of the diode has been already discussed above in section 2.3. Thus, it should be now possible to calculate the resultant dynamic resistance of the diode by following equations,

$$\frac{1}{R_1} = \frac{1}{R_{dif}} + \frac{1}{R_{Sh}} \tag{16}$$

$$\frac{1}{R_2} = \frac{1}{R_{dif}} + \frac{1}{R_{excess}} \tag{17}$$

Eqs. (16) and (17) for the dynamic resistances of the diode respectively correspond to the currents I_1 and I_2 that are described by Eqs. (12) and (13).

3. Results and Discussions

This section presents a discussion of the results obtained from the analysis of I – V characteristics of GaSb-rich superlattice diodes by using the theory outlined in the section 2. Figures 1 and 2 show the reported I–V characteristics of GaSb rich superlattice diodes grown at 450 ^{o}C and 400 ^{o}C respectively [1]. The superlattice period of the active region of the diodes consist of 11 ML × 20 ML of InAs/GaSb layers. Diodes did not have any specifically grown passivation layer except a polymerized film of photoresist to provide protection against the ambient air. The measurement of I–V characteristics was carried out at 77 K by immersing the diode in liquid nitrogen. In Figures 1 and 2 circles show the plot of themeasured diode current versus the applied bias voltage across the diode. We have obtained this data from one of the authors (P. Christol) of the referenced paper [1] on a personal request. It can be also seen from Figures 1 & 2, that the I – V characteristics of samples A and B exhibit a finite current at zero-bias. The observation of the finite zero-bias current of the diodes indicates that the coolant in which the diodes were immersed during measurements is not fully opaque to the background IR radiation from the surrounding objects.

In the present analysis the finite zero-bias current of the diodes has been thus assumed as the background generated photocurrent (I_{Ph}) of the diode. The measured forward characteristics of the diode shown in Figures 1 & 2 were subjected to the best fit to Eqs. (3) to (6) by using the experimentally known value of I_{Ph} and treating the ideality factor η, V_{OC} and R_{Sr} as variable fitting parameters. Primarily for a known value of I_{Ph}, the numerical values of η and V_{OC} determine the variation of the current in the low forward bias region. Similarly, R_{Sr} limits the forward current in the higher bias region. The continuous lines in Figures 1 & 2 are the best fit of the experimental data to the theory.

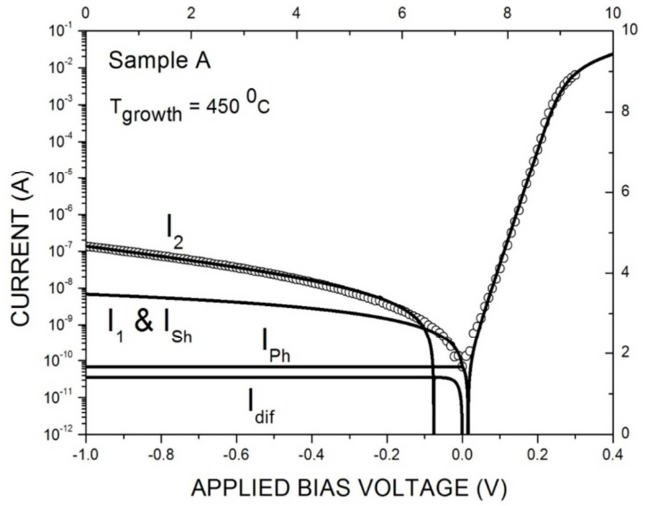

Figure 1. *Measured (open circles) current characteristics of GaSb-rich super lattice diode grown at a temperature of 450 °C and measured at 77 K. Continuous lines show the calculated current components as marked on the respective lines.*

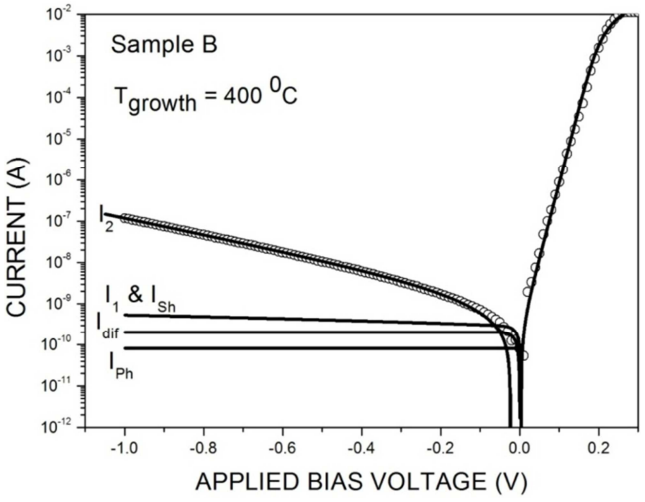

Figure 2. *Measured (open circles) current characteristics of GaSb-rich super lattice diode grown at a temperature of 400 °C and measured at 77 K. Continuous lines show the calculated current components as marked on the respective lines.*

In the reverse bias region of Figures 1 & 2, the continuous line marked with the symbol I_{dif} is the thermal diffusion current contribution, which was calculated from Eq. (2) using the estimated values of I'_{sat} and η from the fitting of the forward characteristics. The continuous line marked with the symbol I_{Ph} is the observed zero-bias current of the diode generated by the background incident IR radiation due to its imperfect cold shielding.

The continuous line marked with the symbol I_{Sh} in the Figures 1 & 2 is the contribution of ohmic shunt current. It was calculated from Eq. (7) by choosing a shunt resistance value that provides the best fit to the diode current in the smaller reverse bias voltage region near zero-bias. The plot of the current I_1, which is the sum of diffusion current, ohmic shunt current and background generated photocurrent overlap the contribution of ohmic shunt current indicating the dominance of ohmic shunt current in the smaller reverse bias region as already discussed in section 2.4.

It can be clearly observed from a comparison of the experimentally observed diode current and the calculated current I_1 that the diodes A and B are exhibiting an excess current in the higher reverse bias region. The line marked as I_2 in Figures 1 & 2 show the excellent fit of the experimental data to Eq. (13) with an important observation that the two terms with in the bracket on the R. H. S. of Eq. (13) exhibit opposite signs. This means that the exponential growth of excess current in the medium and higher reverse bias range takes place by some kind of breakdown process in which both majority and minority carriers (e – h pairs) are produced.

As already mentioned in the section 2.4 the excess diode current is closely related to the value of ohmic shunt resistance. Lower shunt resistance leads to higher excess current. It can be therefore safely proposed that ohmic shunt behaviour at small reverse bias voltages changes to nonlinear behaviour leading to the exponential increase of the current beyond a threshold voltage in the higher reverse bias range. Surface leakage currents are most likely the dominant shunt current in the present case as the diodes under investigation were un-passivated. However, the shunt current contribution from dislocations (if present), which intersect the junction, cannot be ruled out. The nonlinear behaviour of the shunt current leading to the exponential increase of the diode current in the medium and high reverse bias voltage range must be therefore taking place along the shunt current path. In this regard it may be noted from Figures 1 & 2 that the shunt current is the dominant current in both the diodes meaning thereby that a larger part of the diode current is passing through the localized shunt current path which may be either the surface leakage current or the junction intersecting dislocations or partly through both the paths. The current passing through the junction area is relatively much smaller. This physically means that the localized regions of the diode carrying high current density along the shunt current path become more prone to breakdown [21] in the higher reverse bias region leading to the exponential growth of shunt current in its own proportion as suggested by the mathematical derivation of Eq. (8).

It will be now discussed in the following paragraphs that the corresponding R_d–V characteristics of diodes A and B follow very well the present theory of current transport mechanisms described in section 2.5.

Figures 3 & 4 show the R_d-V characteristics of the diodes whose I–V characteristics are shown in Figures 1 & 2, respectively. Circles exhibit the variation of the dynamic resistance as a function of applied bias. All the parameters that were obtained by fitting the current characteristics using the transport current model described in sections 2.1 to 2.4, were used to calculate the dynamic resistance variation of the diodes as detailed in section 2.5.

The continuous lines marked with the letters R_1 and R_2 are the plot of Eqs. (16) and (17). Line marked with R_1 is essentially the plot of theoretically calculated dynamic resistance variation of the diode if the behaviour of the shunt current was of ohmic nature. However, it can be observed

from Figures 3 & 4 that the ohmic behaviour of the shunt current is limited to a small range of reverse bias voltages near zero-bias till the peak of dynamic resistance is arrived. Thereafter for higher reverse bias voltages the dynamic resistance of the diode begins to degrade due to the exponential rise of the current along the shunt current path as seen by the excellent agreement of the experimental data with the theoretically calculated continuous line marked R_2.

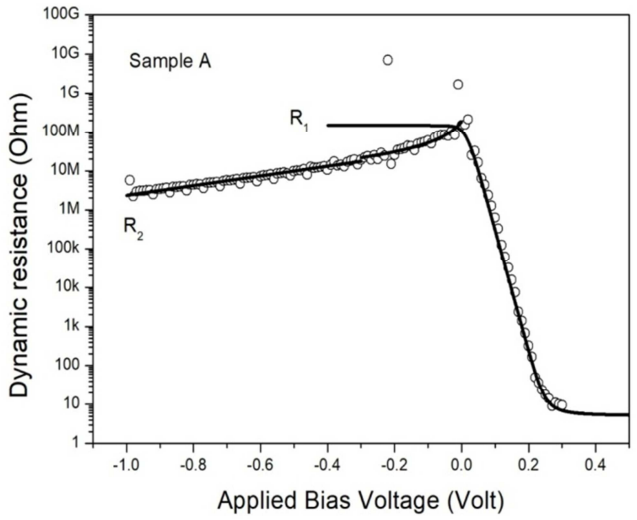

Figure 3. *Dynamic resistance of the diode as a function of applied bias voltage corresponding to I-V characteristics shown in Figure 1. Continuous lines marked R_1 and R_2 exhibit the calculated dynamic resistance corresponding to the currents I_1 and I_2 (shown in Figure 1) after adding the series resistance of the diode. R_1 and R_2 respectively correspond to the ohmic and nonlinear shunt resistance contributions.*

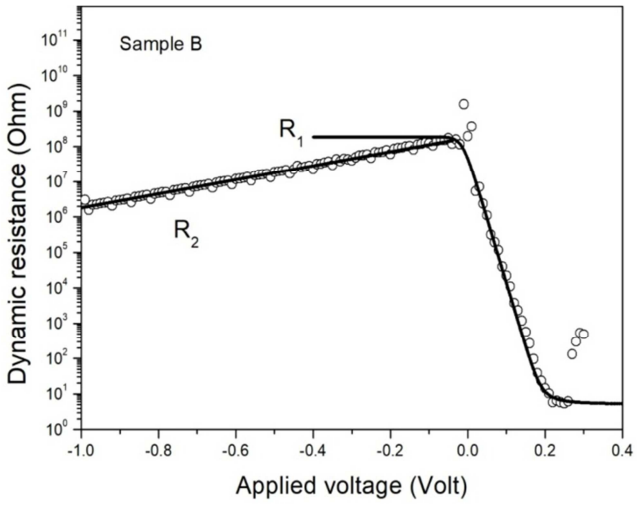

Figure 4. *Dynamic resistance of the diode as a function of applied bias voltage corresponding to I-V characteristics shown in Figure 2. Continuous lines marked R1 and R2 exhibit the calculated dynamic resistance corresponding to the currents I1 and I2 (shown in Figure 2) after adding the series resistance of the diode. R1 and R2 respectively correspond to the ohmic and non-linear shunt resistance contributions.*

4. Summary and Conclusions

Unlike the previous results reported by Delmas et. al. [1], it has been shown in this paper that the behaviour of the electrical characteristics of a GaSb-rich superlattice IR photodiode can be very well explained by taking in to account only the thermal diffusion current, surface leakage (shunt) current and zero-bias current of the diode. The absence of g-r and tunnelling currents in the present analysis can be well understood as the surface leakage current modeled as shunt current is responsible [3, 4] for non-ideal forward characteristics in our model in place of g-r current. Similarly the exponential growth of shunt current is responsible for the excess diode current in the medium and high reverse bias region instead of tunnelling currents. In the present work we have also not used any of the independently measured / known values of the material and diode parameters. In contrast to the conventional models, all the desired parameters used in this model were extracted from the measured I–V characteristic of the given diode itself.

Further in the present study, surface leakage current has emerged as the predominant shunt current of the diode, which exhibits linear dependance on the applied voltage in low reverse bias region near zero-bias but starts exhibiting exponential rise when the reverse bias is increased to medium and high reverse bias voltages. This exponential rise of the current appears to arise from some kind of breakdown process along the shunt current path, in which the current grows in its own proportion and exhibits degradation in the dynamic resistance of the diode, resulting in a peak in the dynamic resistance characteristic.

This paper though has discussed the example of GaSb-rich superlattice diode, the presented model is quite general in nature and is however equally applicable to all types of IR photodiodes irrespective of the material used in their fabrication.

References

[1] Delmas, M., Rodriguez, J. -B., Rossignol, R., Licht, A. S., Giard, E., Mohamed, I. R. and Christol, P. (2016) *J. Appl. Phys.* Vol. 119, 174503.

[2] Taghipour, Z., Lee, S., Myers, S. A., Steenbergen, E. H., Morath, C. P., Cowan, V. M., Mathew, S., Balakrishnan, G. and Krishna, S. (2019) *Appl. Phys. Rev.* Vol. 11, 024047.

[3] Gopal, V., Li, Q., He, J., He, K., Lin, C. and Hu, W., (2016) *J. Appl. Phys.* Vol. 120 084508.

[4] Gopal, V., (2022) *Journal of Electrical and Electronic Engineering* Vol. 20 (5), 180.

[5] Saxena R. S., Saini N. K., Bhan R. K. and Sharma R. K. (2014) *Inf. Phys. Technol.* Vol. 67, 58.

[6] Bhan R. K. and Dhar V. (2019) *Opto-Electronics Review* Vol. 27 (2), 174.

[7] Yang, Q. K., Fuchs, F., Schmitz, J. and Pletschen, W. (2002) *Appl. Phys. Lett.* Vol. 81, 4757 (2002).

[8] Gopal, V., Plis, E., Rodriguez, J. -B. Jones, C. E., Faraone, L. and Krishna, S. (2008) *J. Appl. Phys.* Vol. 104, 124506.

[9] Nguyen, J., Ting, Z., Hill, C. J., Sobel, A., Keo, S. A. and Gunapala, S. D. (2009) *J. Inf. Phys. Technol.* Vol. 52, 317.

[10] Delmas, M., Rodriguez, J. -B. and Christol, P. (2014) *J. Appl. Phys.* Vol. 116, 113101 (2014).

[11] Peng, R., Jiao, S., Jiang, D., Li, H. and Zhao, L. (2017) *Thin Solid Films,* Vol. 629, 55.

[12] Czuba, K., Sankowska, I., Jurenczyk, J., Jasik, A., Papis-Polakowska, E andKaniewski, J., (2017) *Semicond. Sci. Technol.* Vol. (32) No. 5, 055010.

[13] Kim, H. S. (2021) *J. Korean Phys.* Soc. Vol. 78, 1141.

[14] Sah, C. T., Noyce, R. N. and Shockley, W. (1957) *Proc. IRE,* Vol. 45, 1228.

[15] Bhan, R. K., Srivastava, V., Saxena, R. S., Pal, R., Sareen, L. and Sharma, R. K. (2009) *Meas. Sci. Technol.* 20, 117004.

[16] Gopal, V. (2014) *J. Appl. Phys.* Vol. 116, 084502.

[17] Gopal, V., Qiu, W. and Hu, W. (2014) *J. App. Phys.* Vol. 116, 184503.

[18] Gopal, V. and Hu, W. (2015) *J. Appl. Phys.* Vol. 118, 0224503.

[19] Johnson, S. M., Rhiger, D. R., Rosbeck, J. P., Peterson, J. M., Taylor, S. M. and M. E. Boyd, M. E. (1992) *J. Vac. Sci. Technol.* Vol. B10, 1499.

[20] Baker, I. M. and Maxey, C. D., (2001) *J. Electron. Mater.* Vol. 30, 682.

[21] Gopal, V., Gautam, N., Plis, E. and Krishna, S. (2015) *AIP Advances* Vol. 5, 097132.